J. Biophotonics **7**, No. 9, 724–734 (2014) / **DOI** 10.1002/jbio.201300101

Journal of BIOPHOTONICS

FULL ARTICLE

Dynamic molecular monitoring of retina inflammation by *in vivo* Raman spectroscopy coupled with multivariate analysis

Monica Marro[1], *Alice Taubes*[2], *Alice Abernathy*[2], *Stephan Balint*[1], *Beatriz Moreno*[2], *Bernardo Sanchez-Dalmau*[2], *Elena H. Martínez-Lapiscina*[2], *Ivan Amat-Roldan*[2], *Dmitri Petrov*[1,3], *and Pablo Villoslada*[*,2]

[1] ICFO – The Institute of Photonic Sciences, Barcelona, Spain
[2] Center of Neuroimmunology, Institut d'Investigacions Biomèdiques August Pi i Sunyer (IDIBAPS) – Hospital Clinic of Barcelona, Spain
[3] ICREA – Institució Catalana de Recerca i Estudis Avançats, Spain

Received 23 June 2013, revised 20 August 2013, accepted 20 August 2013
Published online 10 September 2013

Key words: Raman spectroscopy, multivariate curve resolution, molecular imaging, neuroinflammation, retina ganglion cells, Multiple Sclerosis

Supporting information for this article is available free of charge under http://dx.doi.org/10.1002/jbio.201300101

Retinal tissue is damaged during inflammation in Multiple Sclerosis. We assessed molecular changes in inflamed murine retinal cultures by Raman spectroscopy. Partial Least Squares-Discriminant analysis (PLS-DA) was able to classify retina cultures as inflamed with high accuracy. Using Multivariate Curve Resolution (MCR) analysis, we deconvolved 6 molecular components suffering dynamic changes along inflammatory process. Those include the increase of immune mediators (Lipoxygenase, iNOS and TNFα), changes in molecules involved in energy production (Cytochrome C, phenylalanine and NADH/NAD+) and decrease of Phosphatidylcholine. Raman spectroscopy combined with multivariate analysis allows monitoring the evolution of retina inflammation.

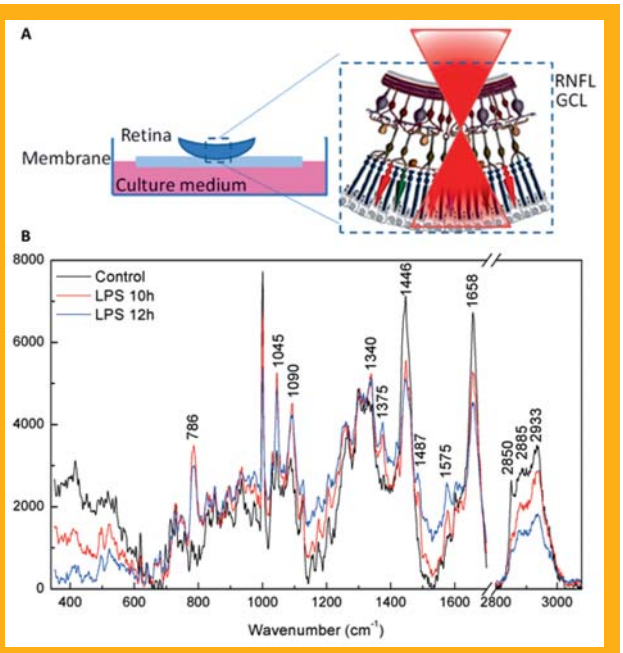

Raman spectroscopy analysis of the Retinal Ganglion Cell layer of the retina. (**A**) Design of the analysis of the Ganglion cell layer (GCL) and Retinal Nerve Fiber Layer (RNFL) of the retina based in the physical properties of laser light and anatomical structure of retinal layers. (**B**) Examples of raw Raman spectra from representative retina sample after 10 hours incubation time (black) and LPS treated retina sample after 10 hours incubation time (red) and 12 hours incubation time (blue).

* Corresponding author: e-mail: pvilloslada@clinic.ub.es

© 2014 by WILEY-VCH Verlag GmbH & Co. KGaA, Weinheim

1. Introduction

The retina is a distinctive component of the central nervous system (CNS) in which retinal ganglion cells from the ganglion cell layer (GCL) project their axons to the brain through the optic nerve and are frequently damaged in several diseases such as Glaucoma and Multiple Sclerosis (MS). Retinal inflammation is primarily mediated by microglia activation, including the release of pro-inflammatory cytokines and the creation of oxidative stress that impairs neuronal function and promotes axonal damage [1–6]. Therefore, the analysis of molecular changes at the retinal level will increase our understanding of neuronal loss and axonal transection, and would aid the development of new neuroprotective strategies for brain and retina diseases.

Raman spectroscopy is a technique that measures the inelastic scattering of photons that occurs when incident light on a sample is transferred into a change in molecular vibrational energy state. Several recent studies have applied this technology to retinal tissue both in animal models and in human subjects in vivo to quantify macular carotenoid pigments [7], advanced glycosilation end products (AGE) levels in Brusch membranes [8], and to differentiate between the molecular content of different retinal layers [9]. Another Raman related technology is coherent anti-Stokes Raman spectroscopy (CARS), which has been applied for obtaining in vivo microscopy images without staining, such as the elucidation of myelin damage in spinal cords following glutamate excitotoxicity in guinea pigs [10].

Although Raman spectroscopy has the maximum specificity among all optical techniques for detecting molecular changes, the interpretation of Raman spectra is complex. Biomolecules have many Raman bands and some of them have similar molecular structures. Consequently, they share groups of bands, making difficult to deconvolute the contributions of pure molecular components from the Raman spectra. During the past decades applications of Raman spectroscopy have been focused to separate several groups of samples by means of multivariate analysis such as Principal Component Analysis (PCA) or to classify samples by Partial Least squares-Discriminant analysis (PLS-DA) or Neural Networks. The aforementioned methods, however, are unable to extract meaningful information that would enable characterization of the Raman spectra of the pure molecules in a sample. For this reason we proposed the application of Multivariate Curve Resolution (MCR) to deconvolute pure molecular components from the Raman spectra and monitor the molecular profile of the tissue over the inflammation process. MCR is an statistical technique that efficiently extracts the information encoded in complex spectra such as those obtained by Raman spectroscopy [11]. Multivariate Curve Resolution – Alternating Least Squares (MCR-ALS) [12] is an unsupervised computational algorithm that iteratively derives the pure component spectra from a spectral data set and the contributions of each pure component in each spectrum acquired [13]. MCR requires minimal a priori knowledge of the system providing objective information. One of the advantages of this method with respect to previously used unmixing algorithms like Vertex Component Analysis (VCA) [12] is the flexibility of the algorithm to include constrains. For instance, physical characteristics of Raman spectra as non-negativity constraints can be included, giving more meaningful component spectra. Thus, MCR represents a novel methodology with promising applicability to study and monitor the biochemical behavior of diseases *in vivo*.

Here we aimed to assess the molecular changes of the GCL over time during retina inflammation by means of Raman spectroscopy. Also, we were interested in obtaining a proof of concept that molecular imaging of the retina by Raman spectroscopy combined with MCR can become a useful technology for studying and monitoring MS and other retina diseases. We made use of an in vitro model of neuroinflammation using murine retinal organotypic cultures, which preserve cellular composition and tissue architecture while allowing direct in vivo imaging analysis [14]. In this study, first we performed a PLS-DA analysis that gave high sensitivity and specificity to discriminate between healthy and inflamed tissue at different stages in the inflammation process. Then, we used Multivariate Curve Resolution (MCR) to deconvolute pure molecular components from the set of experimental Raman spectra that changed during retina inflammation, and we monitored the evolution of their concentrations in the tissue over a 24-hour period process.

2. Methods

2.1 Chemicals

L-glutamic Acid, cytochrome C purified from Pidgeon Breast Muscle, L-(+)-lactic acid, nicotinamide adenine dinucleotide (NADH), L-α-phosphotidylcholine, and N-acetyl-L-aspartic acid (NAA), were purchased from Sigma Aldrich and used without further modification. N-carboxymethyl lysine (CML), and N-carboxyethyl lysine (CEL), and pentosidine were purchased from Polypeptide Laboratories, CML and CEL were used without further modification. Due to packaging constrains, pentosidine was diluted in PBS for analysis. Flavin adenine nucleotide (FAD) was purchased from Carbon

© 2014 by WILEY-VCH Verlag GmbH & Co. KGaA, Weinheim

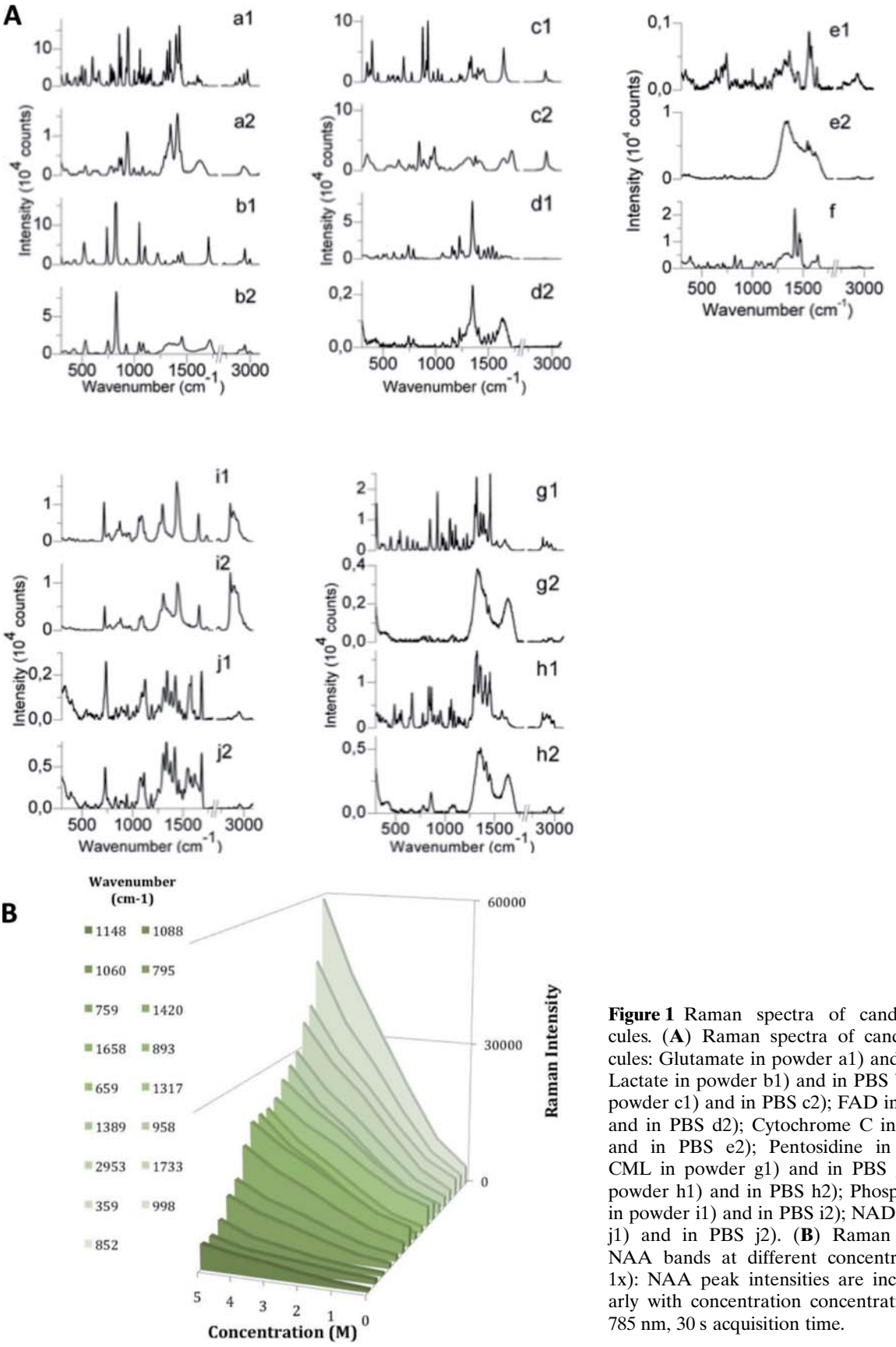

Figure 1 Raman spectra of candidate molecules. (**A**) Raman spectra of candidate molecules: Glutamate in powder a1) and in PBS a2); Lactate in powder b1) and in PBS b2). NAA in powder c1) and in PBS c2); FAD in powder d1) and in PBS d2); Cytochrome C in powder e1) and in PBS e2); Pentosidine in solution f); CML in powder g1) and in PBS g2); CEL in powder h1) and in PBS h2); Phosphatidilcoline in powder i1) and in PBS i2); NADH in powder j1) and in PBS j2). (**B**) Raman intensity of NAA bands at different concentrations (PBS 1x): NAA peak intensities are increasing linearly with concentration concentration 125 mW, 785 nm, 30 s acquisition time.

© 2014 by WILEY-VCH Verlag GmbH & Co. KGaA, Weinheim

Scientific and used without further modification. For the spectra of molecules in solution, powders were mixed with a small amount (1 to 2 drops) of PBS 1x pH 7.4 and imaged at this high concentration, with the exception of NADH which was measured in Triz pH 7.5 due to its documented interactions with the phosphate content of PBS [15]. Eight different concentration of NAA in PBS pH 7 (4 M, 3 M, 2 M, 1 M, 0.5 M, 0.1 M, 0.05 M, and 0.01 M) were prepared by dilution methods. Three to five spectra were taken of each concentration, and spectral intensity versus concentration for each spectral peak was displayed graphically (Figure 1).

2.2 Retina organotypic cultures

Retinal cultures were prepared in accordance with published protocols [16, 17]. Tissue was cultured for six days, then treated with 15 μg/ml lipopolysaccharide (LPS; from Sigma Aldrich) in the tissue culture medium for time periods up to 24 hours as described before [14, 17–19]. Challenged retinas showed microglia activation, axonal damage, production of pro-inflammatory cytokines and oxidative stress (see supplementary methods and Figure S1).

2.3 Raman spectroscopy

Raman spectra were acquired with an InVia Raman microscope from Renishaw with a backscattered configuration. The Raman excitation was performed with 785 nm laser beam focused through a 60X 0.75 NA objective (Leica). Raman spectra for the candidate molecules were obtained by placing the powder or the liquid samples on a sample holder with a cover glass number zero and illuminated from the top with a power from 5 to 40 mW. Retina organotypic cultures were measured using the preparation described above using a power of 100 mW and ensuring no photodamage was induced. The background for all spectra was subtracted using an established method [20]. Background subtraction was implemented in Labview and smoothed using a Butterworth low pass filter and five-point adjacent average. We assigned strong (s), medium (m), and weak (w) labels based on the highest, middle, and lowest third of the peak intensities of each individual spectrum. For individual band assignments no shifts bigger than 10 cm^{-1} were considered. We only assigned a spectrum to a molecule when more than the 90% of the most prominent bands were correlated with the characteristic molecular Raman bands found in the constructed Raman database or in the literature.

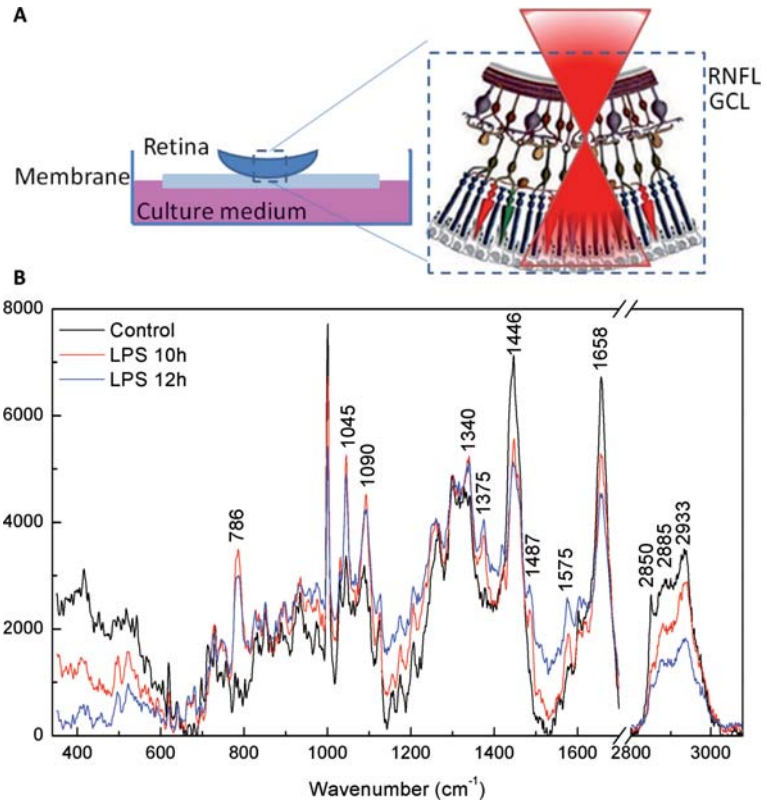

Figure 2 Raman spectroscopy analysis of the Retinal Ganglion Cell layer of the retina. (**A**) Design of the analysis of the Ganglion cell layer (GCL) and Retinal Nerve Fiber Layer (RNFL) of the retina based in the physical properties of laser light and anatomical structure of retinal layers. (**B**) Examples of raw Raman spectra from representative control retina sample after 10 hours incubation time (black) and LPS treated retina sample after 10 hours incubation time (red) and 12 hours incubation time (blue). Highlighted Raman bands undergo visible changes along inflammation that will be further analyzed and quantified by PLS-DA and MCR techniques.

© 2014 by WILEY-VCH Verlag GmbH & Co. KGaA, Weinheim

2.4 Time series and statistical analysis

Spectra were taken randomly from 10 points in the RGC layer of the organotypic retina culture (at a depth of 15–16 μm below tissue surface, Figure 2) in healthy tissue and 2, 4, 6, 8, 10, 12 and 24 hours after LPS challenge. This process was repeated for 6 independent retinas treated with LPS and 6 control retinas. Partial Least Squares – Discriminant Analysis (PLS-DA) was performed using PLS toolbox from Eigenvector Research in MatLab to assess the ability of Raman spectroscopy to discriminate inflamed and control retinas at 10, 12 and 24 hours after LPS challenge. Cross-validation analysis was computed by Venetian blinds (6 bags). The number of retained LVs was chosen to minimize the root mean square error of cross validation (RMSECV) curves.

Principal Component Analysis (PCA) was performed to explore the spectra and select the number of the principal components needed to explain the maximum variance in the data [21]. Once the number of components was identified, the spectra were analyzed by Multivariate Curve Resolution (MCR) as described before [11]. In total, nine components of the spectra were deconvoluted. Three components were identified as background coming from different parts of our system (the culture membrane or residual fluorescence), these components were not used in further analysis. The remaining six components were identified by their respective molecular Raman spectra and tracked through time after LPS challenge induced retina inflammation. Characteristic statistical parameters such as the p value were calculated to assess the significant difference between molecular content in control and LPS challenged tissues. In plots, * signify $p < 0.05$ (significant), ** means $p < 0.01$ (highly significant) and *** is $p < 0.001$ (very highly significant).

3. Results and discussion

3.1 Raman spectra of candidate molecules

We analyzed eight molecules by Raman spectroscopy in powder form and in solution as candidate biomarkers for monitoring retina inflammation. These molecules were selected because they play an important role in neuroinflammation and neurodegeneration. At the same time the molecules showed good signal to noise ratio using Raman spectroscopy. The spectrum of each molecule is presented as spectral library (Figure 1) with an accompanying chart detailing the strength (strong, medium, or weak) of the Raman activity of each peak (supplementary table S1). Of the molecules tested, Glutamate, Lactate, NADH, NAA, Cytochrome C and Phosphatidylcholine presented a good signal to noise ratio in Raman spectra in solution (which better simulates the signal from living tissue, as compared to the powder form) and were used for further analysis. A concentration analysis was carried out on NAA, wherein eight concentrations of this molecule were imaged in solution, and a peak-specific linear regression was carried out in order to characterize the intensity versus concentration curve of each Raman peak. As expected, NAA Raman intensity and concentration was linearly correlated (Figure 1B), supporting the use of Raman signal intensity as a read out of molecular concentration.

3.2 Raman spectra from the GCL of cultured retinas

Spectra were taken at a depth of 11–12 μm from the surface of retina cultures, which given the refractive index of the retinal tissue (reported to be at around 1.35 for murine retina), places the focal point at an actual depth of around 15–16 μm below the tissue surface [22]. The GCL has been shown in adult mice to begin from 13 μm below the surface of the retina in healthy tissue to 3 μm below the surface in tissue with RNFL degradation by inflammation. The average depth of GCL is 40 μm. Taking into account the fact that post-natal p8 mice have less developed tissue structure, our probe focal point at a depth of 15–16 μm was within the GCL, with vertical peripheral data including the entire depth of the RNFL (Figure 2A) [23]. Using this approach we obtained the Raman spectra from murine retina cultures. Figure 2B shows the raw Raman spectra from control tissue and form LPS-treated retinas by 10 and 24 h after challenge. Highlighted bands undergo visible changes over the inflammation. Changes in the spectra were further analyzed by means of PLS-DA and MCR analysis (see below).

3.3 PLS-DA discriminates retina inflammation with high accuracy

Changes in the Raman spectra during the process of neuroinflammation were analyzed from spectra taken at random locations within the central region of each organotypic retina culture at a constant depth of 15–16 μm, putting the focal point within the GCL of the culture. Two independent experiments were performed with 6 retinas per experiment, three retinas were control and three were stimulated with LPS. Ten spectra were taken for each time point and

© 2014 by WILEY-VCH Verlag GmbH & Co. KGaA, Weinheim

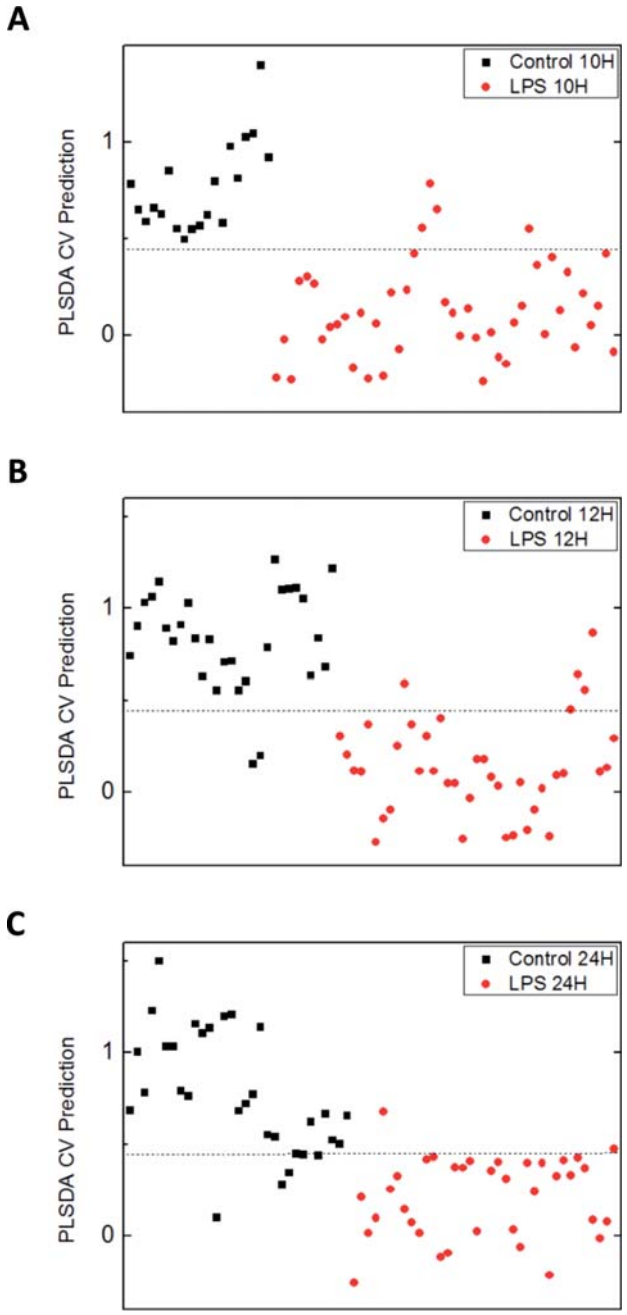

Figure 3 Partial least square – discriminant analysis of Raman spectra in retina cultures in neuroinflammation. A classification model was trained using a PLS-DA algorithm and spectra from control and LPS-stimulated cultures at 10 h, 12 h and 24 h. High accuracy was achieved in the discrimination between healthy and inflammed tissue using cross-validation (sensitivity: 0.91, 0.87 and 0.95, and specificity 1.0, 0.93 and 0.84 for 10, 12 and 24 h respectively). Black squares and red circles represents individual Raman spectra from a point in the retina in control and inflamed tissue respectively. This result shows that Raman spectroscopy coupled with PLS-DA analysis is promising for the detection of neuroinflammation through the retina.

retina. We made use of Partial Least Squares-Discriminant Analysis (PLS-DA) for identifying changes in the Raman spectra associated with retina inflammation. The PLS-DA algorithm was able to classify retina tissue in control or LPS challenged with good accuracy (sensitivity: 0.91, 0.87 and 0.95, and specificity 1.0, 0.93 and 0.84 for 10, 12 and 24 h respectively; Figure 3) using cross-validation (venetian blinds, 6 data splits). Therefore, the fact that the PLS-DA classifier achieved a high accuracy for discriminating between healthy and inflamed tissue support Raman spectroscopy as a tool for monitoring retina inflammation. Also, we identified that the best time to detect inflammatory changes was at 10 h.

3.4 Multivariate Curve Resolution reveals significant changes in molecular components related with immune, energy and lipid mediators during retina inflammation

Based on the good results achieved with PLS-DA algorithm discriminating healthy and inflamed tissue and the fact that Raman spectroscopy has the highest specificity among optical techniques, we attempted to decompose the Raman spectra into meaningful Raman spectra of molecular components changing in concentration along the inflammation using MCR analysis. Nine components were deconvoluted from the spectra by MCR, capturing 99.7% of total variance. Three components were used for background removal from the culture membrane, media and undesired fluorescence. The six remaining components were assigned based on Raman databases or the spectra from our candidate molecules known to have a role in neuroinflammation (see methods).

The first MCR component was tentatively assigned to 5-Lipoxygenase (Figure 4A) based on the Raman spectra found in the Ref. [24] and the agreement between bands. 5-Lipoxygenase is an enzyme involved in metabolism of eicosanoids such as prostaglandins and leukotrienes and therefore critical in the innate immune response. From the reconstructed concentration curve a significant increase of the 5-Lipoxygenase component at 10 to 12 h after LPS challenge was observed. The second component was assigned to iNOS and TNFα (Figure 4B) [25], two well-known proinflammatory molecules involved in CNS inflammation. The temporal evolution of the concentration of iNOS and TNFα components demonstrates a significant increase at 10 hours after LPS application with a maximum at 12 h. Component 3 was assigned to Cytochrome C and Phenylalanine (Figure 4C). This component experienced a

© 2014 by WILEY-VCH Verlag GmbH & Co. KGaA, Weinheim

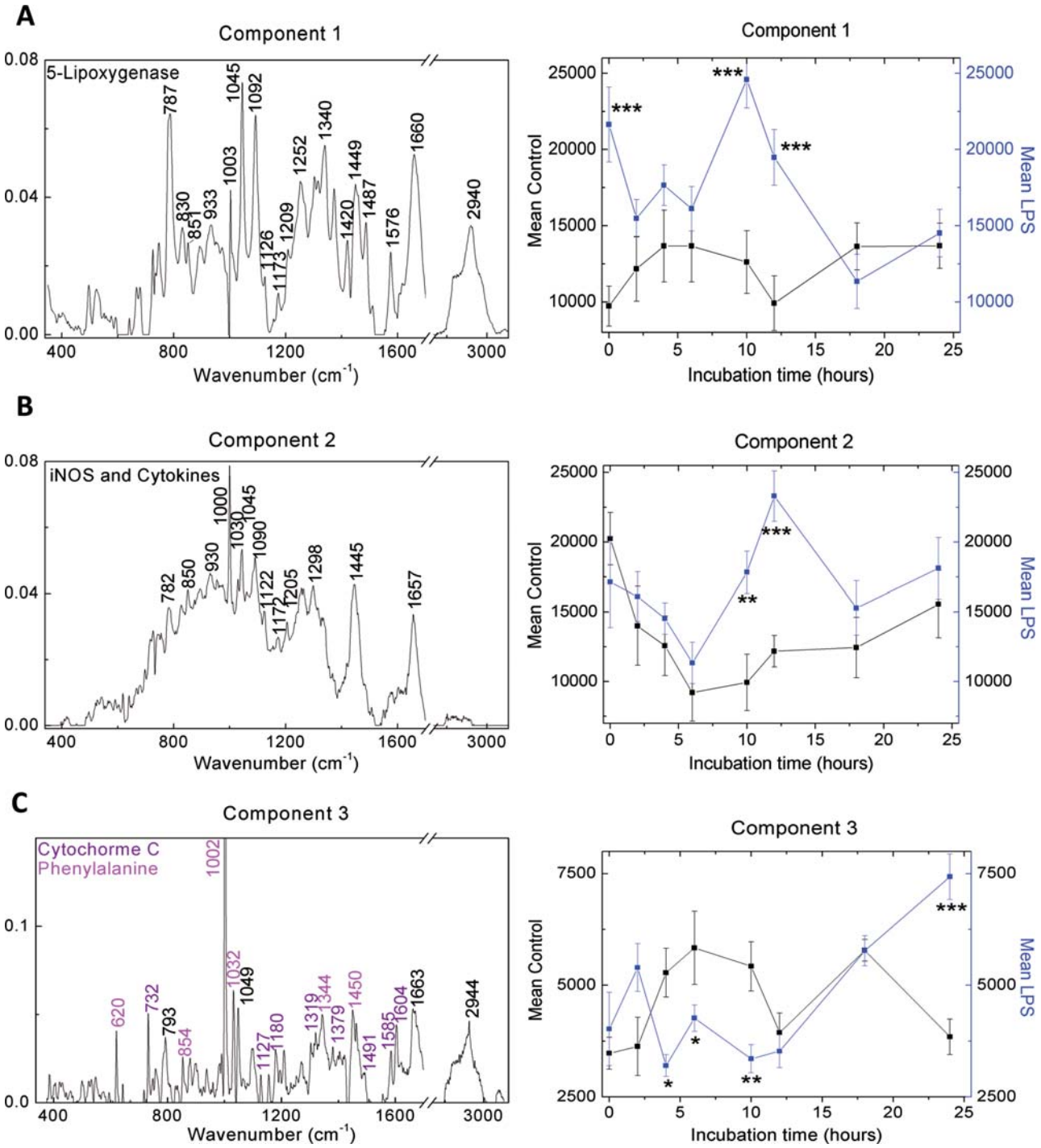

Figure 4 (**A**–**C**)

significant increase in concentration 24 h after the LPS administration. Component 4 was assigned to Phosphatidylcholine (Figure 4D) [26]. The concentration plot showed a significant decrease at 10 to 12 h after LPS challenge compared with baseline. Component 5 contained bands assigned to NAD^+ and NADH (Figure 4E) [27]. The NAD^+/NADH component fluctuates with an early increase by 6 h and decreases 12 h after LPS challenge. The last component (component 6) corresponded to a mixture of molecules, which include several of our candidate molecules including glutamate, NAA, lactate or FAD, as well as structural molecules of the retina present in GCL that do not undergo significant

© 2014 by WILEY-VCH Verlag GmbH & Co. KGaA, Weinheim

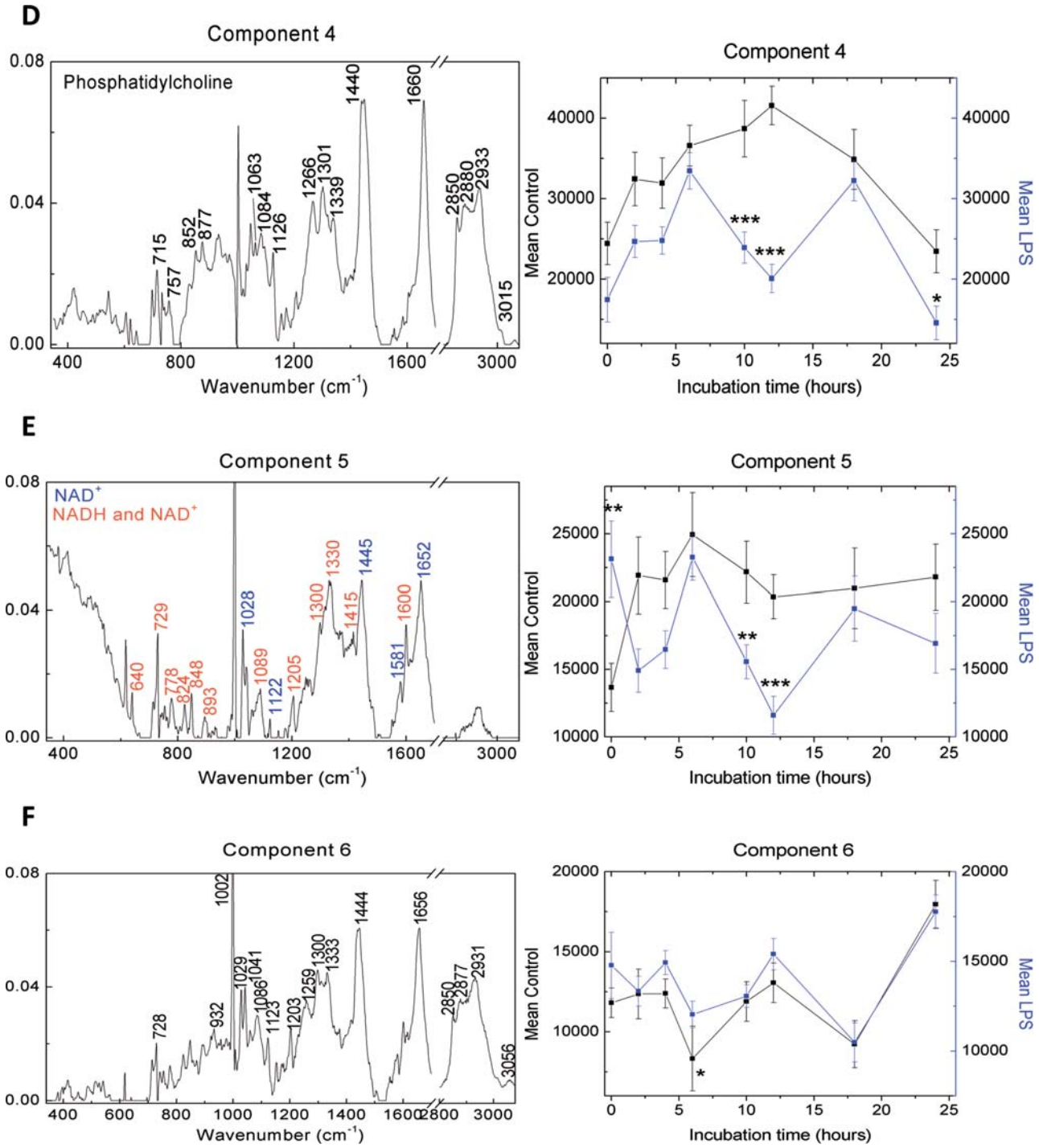

Figure 4 Monitoring the molecular content in retina inflammation by Raman spectroscopy. Molecular components that changed during retina inflammation were deconvolved from the Raman spectra using Multivariate Curve Resolution. The 6 components identified are displayed (**A–F**): a) spectral profile deconvolved for each molecular component; b) Time course of the concentration profile for each molecular component after the LPS challenge. Curves for the mean of the control samples (black line) and the LPS treated samples (blue line) are compared. Error bars are the standard error (SE) that is a measure of how variable the mean will be if you repeat the whole study many times and p values are calculated to show the significance of variations between control and LPS-treated tissue: * $p < 0.05$ (significant), ** $p < 0.01$ (highly significant) and *** $p < 0.001$ (very highly significant).

© 2014 by WILEY-VCH Verlag GmbH & Co. KGaA, Weinheim

changes in concentration during the 24 hours after LPS stimulation (Figure 4F). For this reason they were not further characterized.

4. Discussion

In this study we report the use of Raman spectroscopy of organotypic retinal cultures as a molecular imaging tool to study diseases of the retina. The accessibility of the retina for laser imaging, and the sensitivity of Raman spectroscopy for detecting and quantifying biomolecules, allowed a more detailed study of the temporal evolution of the molecules implicated in neuroinflammation. First, a PLS-DA analysis was performed to construct a mathematical model able to discriminate between the Raman spectra of healthy and inflamed tissue at 10 h, 12 h and 24 h after LPS challenge. A high sensitivity and specificity was achieved predicting the presence of retinal inflammation based on changes in the Raman spectra, suggesting that Raman spectroscopy is a promising tool for molecular monitoring of inflammatory processes in the retina. Second, based on previous results, we monitored the biochemical composition of the retina throughout the inflammatory response. The individual Raman spectra of several molecules were deconvoluted from the complex Raman spectra of the tissue sample; upon deconvolution changes in concentration of important molecules involved in inflammation were observed. By combining biochemical spectra analysis, published Raman databases and multivariate analysis (MCR) we were able to monitor several molecular components that undergo significant changes during retina inflammation. We tentatively assigned those molecular components to Lipoxygenase, iNOS, TNFα, Cytochrome C, Phenyalanine, NADH/NAD+, and Phosphotidylcholine based on our constructed spectral database or Raman spectra published in the literature. Moreover, we provide evidence that quantification of such molecules reflects tissue damage related to retina inflammation. Overall, our results suggest that Raman spectroscopy of the retina combined with PLS-DA and MCR analysis can become a useful molecular imaging technique for the detection, study and monitoring of retina and brain diseases.

The molecular components deconvoluted by MCR of Raman spectra of LPS treated retina point to important molecular players in the process of neuroinflammation in the CNS. The enzyme Lipoxygenase is associated with the production of leukotrienes, which are associated with inflammation of brain tissue mediated by the innate immune system [28]. In the cycle of neuroinflammation and oxidative stress in the central nervous system, iNOS plays a critical role exacerbating the hypoxic environment through overproduction of nitric oxide (NO). The production of $NO^{\bullet}$ by iNOS has deleterious effects on the electron transport chain, and is a major cause of neuronal and axonal damage [14]. The pro-inflammatory cytokine TNF-α is a key component of the signaling cascade associated with the inflammatory response in nervous tissue resulting in cellular damage [29]. Oxidative stress can significantly interfere with the electron transport and mitochondrial function, promoting the export of Cytochrome C to the cytoplasm, which is an important trigger for cell death [30]. In addition, NAD seems to play a significant role in the control of the autoimmune attack against the brain in MS through the regulation of the enzyme indoleamine 2,3-dioxygenase (IDO), regulating T cell activation but also the interaction between neurons and microglia [31]. The anoxic cellular environment, in which cells must rely primarily on glycolysis to generate ATP, will increase NADH levels, while decreasing NAD+ supplies. The increased levels of NO impair the electron transport chain, without which NAD+ levels are unable to be maintained. Fluctuations of these metabolites may reflect metabolic stress experienced by the retina during inflammation. The role of Phenylalanine is complex, it is a precursor of tryptophan and kynurenins which play an important role in the control of endogenous regulation of neuronal excitability and initation of immune tolerance [32], and is known to play a role in modulating the stability of myelin during neuroinflammation [33].

The combination of molecular imaging by Raman spectroscopy with advanced imaging modalities of the retina such as spectral domain optical coherence tomography (OCT) will provide valuable insights into the pathological events in retina inflammation. For example, in the case of MS, damage of the retina in absence of optic neuritis is a phenomenon observed from the early stages of the disease progression [34–35]. The molecular basis of this phenomenon is not understood; however, it is hypothesized that in patients with MS grey matter and the retina suffer chronic and diffuse inflammatory processes, which damage retinal neurons. The application of Raman spectroscopy focused in the retinal layers damaged by MS would reveal the molecular changes occurring and better characterize MS pathogenesis. The translation of Raman spectroscopy to human use is not introducing additional safety concerns, unless limiting the time of analysis. The clinical applications of Raman spectroscopy could be broad, especially when combined with scanning laser ophthalmoscope or OCT.

Several limitations would need be overcome to fully apply this technique in the clinical setting. We studied the changes induced by LPS in an *in vitro* model of retinal inflammation in which timing and location were well controlled. In humans, however,

© 2014 by WILEY-VCH Verlag GmbH & Co. KGaA, Weinheim

changes in immune mediators may be more difficult to detect due to heterogeneity between subjects. Furthermore, the changes observed are the result of a chronic process rather than an acute challenge, making it more difficult to identify patterns observed *in vitro*. For these reasons we plan to analyze changes in retinas from mice suffering optic neuritis resulting from Experimental Autoimmune Encephalomyelitis, a well-known model of MS. Second, the specificity of the assignment of spectra to molecules (we required a 90% band coincidence) does not completely preclude the possibility that the signal identified may come from other molecules, in addition to the ones suggested. Potential band overlap points to the concomitant use of techniques like ELISA or High-performance liquid chromatography (HPLC) with other disease models of MS. At present, validation using these techniques is difficult because it is complicated to find a technique able to validate Raman results because with this technique we are monitoring the molecular composition of the tissue in a small volume and in the order of microns over a period of time while the tissue is undergoing chemical changes. Other techniques are invasive and measure the overall concentration in the tissue, rather than in a specific layer of the tissue (HPLC). Also, the identification of the molecules that significantly change in our study were based in the characterization of a set of candidate molecules and the information available in Raman databases, which is limited at present. For this reason, future research improving the database of Raman spectra of biomolecules, would allow better identification of molecular changes by this technology. Finally, Raman spectroscopy is limited in its ability to accurately distinguish isoforms or posttranslational modifications of a given molecule, these modifications may be of great importance for several biological processes.

5. Conclusion

Raman spectroscopy combined with MCR analysis is an unbiased screening technique that identifies temporal changes in any molecule present in the spectra. The use of Raman spectroscopy to analyze findings in inflamed and control retina cultures has revealed several peaks of interest within the retinal spectra that can be attributable to changes in inflammatory mediators, components of the mitochondria and fatty acids during neuroinflammation. Further research is required to characterize the behavior of the Raman bands of these molecular components as a function of disease progress, and to apply this technique as a diagnostic tool. In summary, Raman spectroscopy of the retina may become a promising application to study retina diseases *in vivo*.

Acknowledgements This work was supported by the Generalitat de Catalunya (PROVA'T-2011–007, co-financed by 2007–2013 Catalonia OP ERDF, a way of Building Europe); Instituto de Salud Carlos III: PS09/00259 and Red Española de Esclerosis Multiple (RD07/0060/001) to PV; and FIS2008–00114 to DP; and by the Fundació Cellex to both centers.

Disclosure Authors have no conflict of interest with current research. PV is founder and hold stocks in Bionure Farma SL. PV has received consultancy fees from Novartis, Roche, MedImmune, Digna Biotech, Neurotec Farma, Bionure Farma and Heidelberg Engineering.

Author biographies Please see Supporting Information online.

References

[1] P. Yang, A. F. de Vos, and A. Kijlstra, Invest Ophthalmol Vis Sci, **37**, 77–85 (1996).
[2] B. Detrick and J. J. Hooks, Immunol Res, **47**, 153–161 (2010).
[3] C. Kaur, G. Rathnasamy, and E. A. Ling, J Neuroimmune Pharmacol, **8**, 66–78 (2013).
[4] A. Ebneter, R. J. Casson, J. P. Wood, and G. Chidlow, Invest Ophthalmol Vis Sci, **51**, 6448–6460 (2010).
[5] K. S. Shindler, E. Ventura, M. Dutt, and A. Rostami, Exp Eye Res, **87**, 208–213 (2008).
[6] P. Yang, L. Chen, R. Zwart, and A. Kijlstra, Invest Ophthalmol Vis Sci, **43**, 1488–1492 (2002).
[7] I. V. Ermakov, M. Sharifzadeh, M. Ermakova, and W. Gellermann, J Biomed Opt, **10**, 064028 (2005).
[8] J. V. Glenn, J. R. Beattie, L. Barrett, N. Frizzell, S. R. Thorpe, M. E. Boulton, J. J. McGarvey, and A. W. Stitt, FASEB J, **21**, 3542–3552 (2007).
[9] J. R. Beattie, S. Brockbank, J. J. McGarvey, and W. J. Curry, Mol Vis, **13**, 1106–1113 (2007).
[10] Y. Fu, W. Sun, Y. Shi, R. Shi, and J. X. Cheng, PloS ONE, **4**, e6705 (2009).
[11] Patel, II, J. Trevisan, G. Evans, V. Llabjani, P. L. Martin-Hirsch, H. F. Stringfellow, and F. L. Martin, Analyst, **136**, 4950–4959 (2011).
[12] J. Jaumota, R. Gargalloa, A. de Juana, and R. Tauler, Chemom Intel Lab Syst, **76**, 101–110 (2005).
[13] M. Garrido, F. X. Rius, and M. S. Larrechi, Anal Bioanal Chem, **390**, 2059–2066 (2008).
[14] A. Di Penta, B. Moreno, S. Reix, B. Fernandez-Diez, M. Villanueva, O. Errea, N. Escala, K. Vandenbroeck, J. X. Comella, and P. Villoslada, PloSONE, **8**, e54722 (2013).
[15] L. Rover, Junior, J. C. Fernandes, G. de Oliveira Neto, L. T. Kubota, E. Katekawa, and S. H. Serrano, Anal Biochem, **260**, 50–55 (1998).

© 2014 by WILEY-VCH Verlag GmbH & Co. KGaA, Weinheim

[16] M. Donovan, F. Doonan, and T. G. Cotter, Dev Biol, **291**, 154–169 (2006).
[17] K. Mertsch, U. K. Hanisch, H. Kettenmann, and J. Schnitzer, J Comp Neurol, **431**, 217–227 (2001).
[18] C. Broderick, L. Duncan, N. Taylor, and A. D. Dick, Invest Ophthalmol Vis Sci, **41**, 2613–2622 (2000).
[19] W. Y. Wang, G. Z. Xu, J. Tian, and A. J. Sprecher, Curr Eye Res, **34**, 476–484 (2009).
[20] T. J. Romer, J. F. Brennan, 3rd, M. Fitzmaurice, M. L. Feldstein, G. Deinum, J. L. Myles, J. R. Kramer, R. S. Lees, and M. S. Feld, Circulation, **97**, 878–885 (1998).
[21] M. Hedegaard, C. Krafft, H. J. Ditzel, L. E. Johansen, S. Hassing, and J. Popp, Anal Chem, **82**, 2797–2802 (2010).
[22] A. Ajo, Acta Physiol Scand, **13**, 130–149 (1947).
[23] X. Zhang, A. Chaudhry, and S. K. Chintala, Mol Vis, **9**, 238–248 (2003).
[24] P. Guthikonda, J. Baker, and D. H. Mattson, J Neuroimmunol, **82**, 133–139 (1998).
[25] L. L. Hua, J. S. Liu, C. F. Brosnan, and S. C. Lee, Ann Neurol, **43**, 384–387 (1998).
[26] V. C. Stewart, G. Giovannoni, J. M. Land, W. I. McDonald, J. B. Clark, and S. J. Heales, J Neurochem, **68**, 2547–2551 (1997).
[27] D. Chen, K. T. Yue, C. Martin, K. W. Rhee, D. Sloan, and R. Callender, Biochemistry, **26**, 4776–4784 (1987).
[28] H. E. de Vries, M. Witte, D. Hondius, A. J. Rozemuller, B. Drukarch, J. Hoozemans, and J. van Horssen, Free Radic Biol Med, **45**, 1375–1383 (2008).
[29] J. N. Ratchford, S. Saidha, E. S. Sotirchos, J. A. Oh, M. A. Seigo, C. Eckstein, M. K. Durbin, J. D. Oakley, S. A. Meyer, A. Conger, T. C. Frohman, S. D. Newsome, L. J. Balcer, E. M. Frohman, and P. A. Calabresi, Neurology, **80**, 47–54 (2013).
[30] M. Politis, P. Giannetti, P. Su, F. Turkheimer, S. Keihaninejad, K. Wu, A. Waldman, O. Malik, P. M. Matthews, R. Reynolds, R. Nicholas, and P. Piccini, Neurology, **75,** 523–530 (2012).
[31] W. T. Penberthy and I. Tsunoda, Curr Pharm Des, **15**, 64–99 (2009).
[32] B. Stankoff, L. Freeman, M. S. Aigrot, A. Chardain, F. Dolle, A. Williams, D. Galanaud, L. Armand, S. Lehericy, C. Lubetzki, B. Zalc, and M. Bottlaender, Ann Neurol, **69**, 673–680 (2011).
[33] J. Versijpt, J. C. Debruyne, K. J. Van Laere, F. De Vos, J. Keppens, K. Strijckmans, E. Achten, G. Slegers, R. A. Dierckx, J. Korf, and J. L. De Reuck, Mult Scler, **11**, 127–134 (2005).
[34] J. M. Gelfand, D. S. Goodin, W. J. Boscardin, R. Nolan, A. Cuneo, and A. J. Green, Retinal axonal loss begins early in the course of multiple sclerosis and is similar between progressive phenotypes. PLoS One. 7, e36847 (2012).
[35] T. Oberwahrenbrock, M. Ringelstein, S. Jentschke, K. Deuschle, K. Klumbies, J. Bellmann-Strobl, J. Harmel, K. Ruprecht, S. Schippling, H. P. Hartung, O. Aktas, A. U. Brandt, and F. Paul, Retinal ganglion cell and inner plexiform layer thinning in clinically isolated syndrome. Mult Scler. 2013 May 23. [Epub ahead of print] PubMed PMID: 23702433.

© 2014 by WILEY-VCH Verlag GmbH & Co. KGaA, Weinheim